



**HAL**  
open science

# Nonlinear instabilities driven by coherent phase-space structures

Maxime Lesur, P. Diamond

► **To cite this version:**

Maxime Lesur, P. Diamond. Nonlinear instabilities driven by coherent phase-space structures. *Physical Review E : Statistical, Nonlinear, and Soft Matter Physics* [2001-2015], 2013, 87 (3), <10.1103/physreve.87.031101>. <hal-01969766>

**HAL Id: hal-01969766**

**<https://hal.science/hal-01969766v1>**

Submitted on 14 Jan 2019

**HAL** is a multi-disciplinary open access archive for the deposit and dissemination of scientific research documents, whether they are published or not. The documents may come from teaching and research institutions in France or abroad, or from public or private research centers.

L'archive ouverte pluridisciplinaire **HAL**, est destinée au dépôt et à la diffusion de documents scientifiques de niveau recherche, publiés ou non, émanant des établissements d'enseignement et de recherche français ou étrangers, des laboratoires publics ou privés.



HAL Authorization

## Nonlinear instabilities driven by coherent phase-space structures

M. Lesur<sup>1,2</sup> and P. H. Diamond<sup>1,3</sup>

<sup>1</sup>*WCI Center for Fusion Theory, NFRI, Gwahangno 113, Yuseong-gu, Daejeon 305-333, Korea*

<sup>2</sup>*Itoh Research Center for Plasma Turbulence, Kasuga, Kasuga Koen 6-1, 816-8580, Kyushu University, Japan*

<sup>3</sup>*CMTFO and CASS, University of California, San Diego, La Jolla, California 92093, USA*

(Received 20 February 2012; revised manuscript received 7 May 2012; published 12 March 2013)

In the presence of wave dissipation, phase-space structures emerge in nonlinear Vlasov dynamics. Our theory gives a simple relation between the growth of these coherent structures and that of the wave energy. The structures can drive the wave by direct momentum exchange, which explains the existence of nonlinear instabilities in both barely unstable and linearly stable (subcritical) regimes. When dissipation is modeled by a linear term in the field equation, simple expressions of a single-hole growth rate and of the initial perturbation threshold are in agreement with numerical simulations.

DOI: [10.1103/PhysRevE.87.031101](https://doi.org/10.1103/PhysRevE.87.031101)

PACS number(s): 52.35.Mw, 05.65.+b, 52.35.Sb

Instability dynamics [1,2] is of great interest in the context of pattern formation [3], the onset of turbulence [4], and many other subjects. While instabilities are central to virtually every field of physics, in collisionless or weakly collisional plasmas the disparate roles of resonant and nonresonant particles offers an interesting variation on time-honored methods and approaches. In this respect, it has long been realized that wave and instability dynamics and evolution in a collisionless plasma can be described in terms of coupled, interpenetrating ensembles of resonant and nonresonant particles or, equivalently, resonant particles and a gas of plasmon quasiparticles. While the linear theory of the Vlasov plasma is well established, its nonlinear theory is a rich and still-evolving subject. Rather little, however, is understood about nonlinear, or subcritical, Vlasov stability, in which the growth process circumvents linear theory [5]. One idea concerning subcritical processes derives from the properties of phase-space granulations or structures, which can exchange momentum via channels which differ from that of familiar wave-particle resonance, and so can tap free energy when wave excitation cannot [6]. Such granulations are self-bound aggregations of resonant particles, which constitute a novel collective exciton. In this Rapid Communication, we present a theory of subcritical Vlasov plasma instability formulated in terms of the evolution of waves and phase-space density correlations. Not surprisingly, the theory for one-dimensional (1D) Vlasov plasmas has considerable overlap with those describing the evolution of flows in a quasigeostrophic fluid. Both are two-dimensional (2D) systems which support waves, and are constrained by two invariants: energy and enstrophy in the fluid case, wave energy and phasestrophy in the Vlasov case. The mechanisms involved are relevant to many laboratory and space plasmas, in particular, in the context of energetic particle interaction with Alfvén waves, collisionless trapped electron modes, and trapped ion ITG instabilities.

To illustrate our theory, we choose two simple models that treat one-dimensional plasmas. The first model is the bump-on-tail instability, which is a fundamental paradigm for the basic process of Langmuir waves driven by a suprathermal population. The Berk-Breizman (BB) extension of the bump-on-tail model includes an external wave damping  $\gamma_d$  to account for linear dissipative mechanisms of the wave energy to the

background plasma [7]. The second model is the current-driven ion-acoustic (CDIA) instability, which is a fundamental paradigm for sound waves driven by a velocity drift between thermal ions and thermal electrons. In both models, finite wave damping (externally applied in the BB model; due to ion Landau damping in the CDIA model) allows for the spontaneous creation of self-trapped structures (called holes and clumps) in the 2D phase space, whose median velocity evolves in time, resulting in spectral components with a frequency shift  $\delta\omega(t)$  (chirping). The growth of phase-space structures results from momentum exchange between the structure and the wave, or between species, which is due to the dissipation acting on structures. The evolution of holes and clumps is a self-organization process, which provides the energy required to balance dissipation.

Subcritical instabilities have been observed in BB simulations [7,8] and CDIA simulations [9]. Based on the theory, we explain the mechanism of subcritical instabilities as follows. Landau damping generates a seed phase-space structure, whose growth rate can be positive if the growth due to momentum exchange overcomes decay due to collisions. In addition, our theory predicts the persistence of nonlinear instability in the marginally linear unstable regime. The theoretical arguments are in good agreement with results from high resolution numerical simulations.

For the first model, we adopt a perturbative approach, and cast the BB model in a reduced form, which describes the time evolution of the beam particles only [7,10]. In this sense, we note that the BB model with extrinsic dissipation is also applicable to the traveling wave tube “quasilinear experiment” with a lossy helix [11]. In this model, a single electrostatic wave with a wave number  $k$  is assumed and the real frequency of the wave is set to  $\omega = \omega_p$ , the Langmuir plasma frequency. The evolution of the beam distribution,  $f(x, v, t)$ , is given by a kinetic equation

$$\frac{\partial f}{\partial t} + v \frac{\partial f}{\partial x} + \frac{qE}{m} \frac{\partial f}{\partial v} = -v_a \delta f + \frac{v_f^2}{k} \frac{\partial \delta f}{\partial v} + \frac{v_d^3}{k^2} \frac{\partial^2 \delta f}{\partial v^2}, \quad (1)$$

where  $\delta f \equiv f - f_0$ , and  $f_0(v)$  is the initial velocity distribution. The evolution of the pseudoelectric field  $E \equiv Z \exp i\zeta +$

c.c. is given by

$$\frac{dZ}{dt} = -\frac{m\omega_p^3}{4\pi q n_0} \int f(x, v, t) e^{-i\zeta} dx dv - \gamma_d Z, \quad (2)$$

where  $\zeta \equiv kx - \omega t$ , and  $n_0$  is the total density.

For the second model, we include two species  $s = i, e$ , assume collisions are negligible, and do not filter a particular wave number. The CDIA model is composed of two kinetic equations,  $\partial_t f_s + v \partial_x f_s + (q_s/m_s) E \partial_v f_s = 0$ . and a current equation,

$$\frac{\partial E}{\partial t} = -\frac{m\omega_p^2}{n_0 q^2} \sum_s \int v f_s(x, v, t) dv. \quad (3)$$

We use the COBBLES code [8] to solve the initial-value problems described above. In BB simulations, the velocity distribution  $f_0$  is designed with a constant slope such that  $\gamma_{L0}/\omega = 0.1$  [12], where  $\gamma_{L0} = (\pi\omega^3)/(2k^2 n_0) \partial_v f_0$  is a measure of the slope such that  $\gamma \sim \gamma_{L0} - \gamma_d$ . In CDIA simulations, the initial velocity distributions  $f_{0,s}$  are two Gaussians with thermal velocity  $v_{th,s}$  centered at  $v = v_s$ . We choose  $m_i = 4m_e$ ,  $v_{th,e} = 2v_{th,i}$  ( $T_e = T_i$ ), and a drift  $(v_e - v_i)/v_{th,i} = 3$ , which is below the linear CDIA stability threshold (3.92).

The equations below can be applied to the BB case by removing the subscript  $s$ , or to the CDIA case by taking  $\gamma_d = v_a = v_f = v_d = 0$ . The evolution of phase-space structures follows that of the phasestrophy [13,14],

$$\Psi_s \equiv \int_{-\infty}^{\infty} \langle \delta f_s^2 \rangle dv, \quad (4)$$

where the angle brackets denote the spatial average.

Simple algebra yields an exact relation for the evolution of phasestrophy,

$$\frac{d\Psi_s}{dt} = -2\frac{q_s}{m_s} \int_{-\infty}^{\infty} \frac{df_{0,s}}{dv} \langle E \delta f_s \rangle dv - \gamma_{\Psi}^{\text{col}} \Psi_s, \quad (5)$$

where  $\gamma_{\Psi}^{\text{col}}$  is the decay rate of phasestrophy due to collisions,

$$\gamma_{\Psi}^{\text{col}} = 2v_a + \frac{2}{\Psi_s} \frac{v_d^3}{k^2} \int_{-\infty}^{\infty} \left\langle \left( \frac{\partial \delta f_s}{\partial v} \right)^2 \right\rangle dv. \quad (6)$$

Note that collisional drag  $v_f$  does not appear in the latter expression.

The wave energy equation is

$$\frac{dW}{dt} + 2\gamma_d W = -2 \sum_s u_s q_s \int \langle E \delta f_s \rangle dv, \quad (7)$$

where  $W = n_0 q^2 \langle E^2 \rangle / (m\omega_p^2)$  is the total wave energy, including sloshing energy. In the BB case,  $u_s = \omega_p / (2k)$ . In the CDIA case, we assumed that the dominant phase-space structures are localized in a neighborhood of  $v = u_s$ . We assume that  $f_{0,s}$  has a constant slope in the velocity range spanned by evolving phase-space structures. Then, phasestrophy evolution is linked to the wave energy evolution by

$$\frac{dW}{dt} + 2\gamma_d W = \sum_s \frac{m_s u_s}{d_v f_{0,s}} \left( \gamma_{\Psi}^{\text{col}} + \frac{d}{dt} \right) \Psi_s. \quad (8)$$

In parallel with quasigeostrophic fluids, this relation is the kinetic counterpart of the Charney-Drazin nonacceleration theorem [15]. Figure 1 shows good quantitative agreement

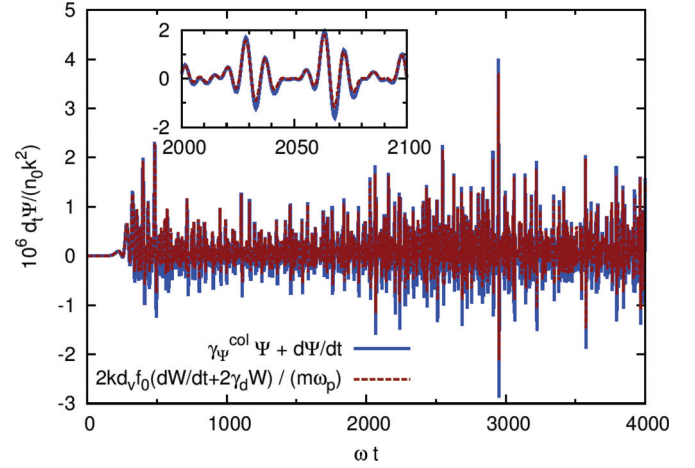


FIG. 1. (Color online) Growth of phasestrophy and wave energy in the BB case. Inset: Zoom on a smaller time scale. Simulation parameters are  $\gamma_{L0}/\omega = 0.1$ ,  $\gamma_d/\gamma_{L0} = 0.7$ ,  $v_a/\gamma_{L0} = 10^{-3}$ , and  $v_f = v_d = 0$ .

between the left-hand side (lhs) and the right-hand side (rhs) in a BB simulation. Figure 2 shows qualitative agreement between the lhs and the rhs in a CDIA simulation, where we have replaced  $u_s$  by the velocity of maximum overlap between  $f_{0,i}$  and  $f_{0,e}$ ,  $u_s = 1.42v_{th,i}$ . For  $\omega_{pe}t < 1000$ , structures are not localized around  $v = u_s$ , which accounts for the discrepancy. Since phasestrophy is directly related to the perturbed momentum in the collisionless limit,  $\Psi_s = -2d_v f_{0,s} \int v \langle \delta f_s \rangle dv$ , phasestrophy growth implies an exchange of momentum, between structures and waves, or between species.

In the BB case, we can apply the above general theory to obtain an expression for the nonlinear growth rate of an isolated phase-space structure. We assume that  $\delta f$  is of the form  $\delta f = \langle \delta f \rangle [1 + \cos(kx + \theta)]$ , with a Gaussian profile,  $\langle \delta f \rangle = h(t) \exp\{-[v - v_0(t)]^2 / [2\Delta v(t)^2]\}$ . This shape corresponds to a Bernstein-Green-Kruskal mode, which was shown to be a state of maximum entropy subject to constant mass, momentum, and energy [6]. To relate  $W$  to  $\Psi$ , we use the Poisson equation, even though (in the BB model) it is only

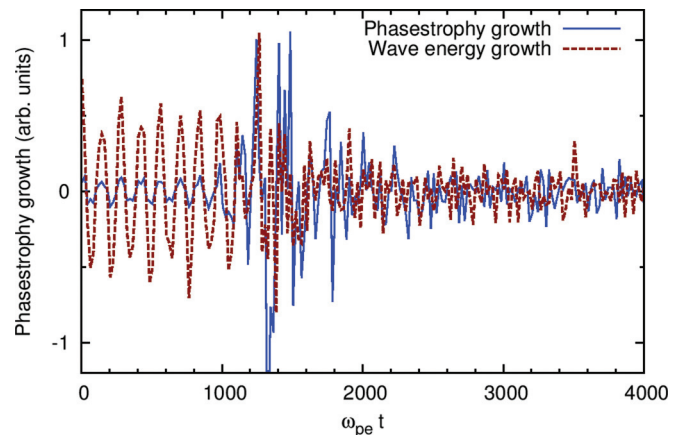


FIG. 2. (Color online) Growth of phasestrophy and wave energy in the CDIA case.

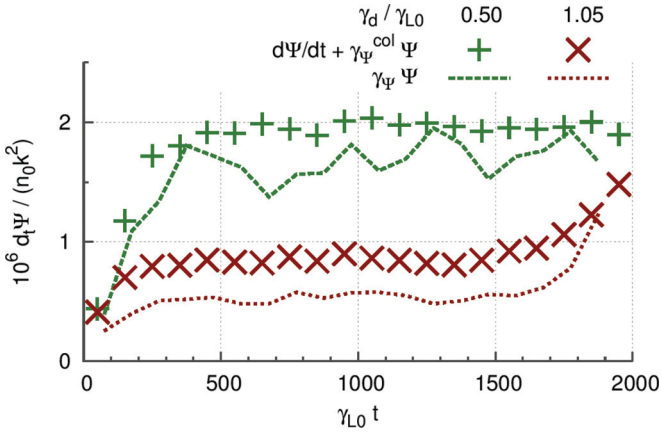


FIG. 3. (Color online) Growth rate of the phasestrophy of one isolated hole. Simulation parameters are  $\gamma_{L0}/\omega = 0.1$ ,  $v_a = 0$ ,  $v_f/\gamma_{L0} = 0.3$ ,  $v_d/\gamma_{L0} = 0.17$ , and two different values of  $\gamma_d$ , which are given in the legend. Points: Phasestrophy growth measured in simulations, including a contribution from collisions. Dashed curves: Theory, Eq. (10).

approximately satisfied,

$$W = \frac{1}{2} \frac{m\omega_p^2}{k^2 n_0} \left( \int \langle \delta f \rangle dv \right)^2. \quad (9)$$

Thus the evolution of phasestrophy follows a simple expression,  $d\Psi/dt = (\gamma_{\Psi} - \gamma_{\Psi}^{\text{col}}) \Psi$ , where  $\gamma_{\Psi}$  is the collisionless phase-space structure growth rate,

$$\gamma_{\Psi} \approx \frac{16}{3\sqrt{\pi}} \frac{\Delta v}{v_R} \frac{\gamma_{L0}}{\omega_p} \gamma_d. \quad (10)$$

To be concise, in this expression for  $\gamma_{\Psi}$  we assumed  $\Delta v v_f \ll kn_0/\omega$  and  $\Delta v \ll \gamma_d \Delta v$ , which are satisfied in our simulations. Equation (10) is in qualitative agreement with the collisionless structure growth rate estimated in Ref. [16]. However, the method used in the reference assumes that  $\partial E_0/\partial t \ll \gamma_d E_0$ , which is only valid in the initial, linear phase, near marginal stability. Figure 3 shows the growth of phasestrophy, averaged over a time window of duration  $\gamma_{L0} \Delta t = 100$ , where  $\Delta v$  in the expression of  $\gamma_{\Psi}$  is estimated by fitting a Gaussian to  $\langle \delta f \rangle$  in the vicinity of the hole at each time step. We observe quantitative agreement between our simulations and theory for the supercritical case ( $\gamma_d/\gamma_{L0} = 0.5$ ), and qualitative agreement in the subcritical case ( $\gamma_d/\gamma_{L0} = 1.05$ ). There is a 40% discrepancy in the subcritical case, which is due in part to the coexistence of a secondary hole with 20% as much phasestrophy as that of the main hole. This suggests that consideration of the primary-secondary hole interaction is necessary to improve the accuracy of the theory.

Equation (10) shows that the growth of structures is independent of linear stability, since it is not related to the sign of the total linear growth rate  $\gamma \approx \gamma_{L0} - \gamma_d$ . Nonlinear growth requires a positive  $\gamma_d$  to enable momentum exchange, a positive slope for  $f_0$  to provide free energy, and a seed structure with a width  $\Delta v$  large enough for  $\gamma_{\Psi}$  to overcome collisions. When the linear growth rate  $\gamma$  is negative, the seed structure is the hole (clump) corresponding to the  $v > v_R$  ( $v < v_R$ ) part of the plateau, which is formed by particles trapped in the finite initial electric field. Subcritical instabilities have

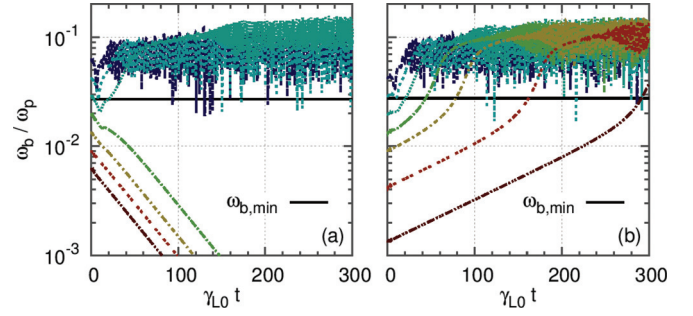


FIG. 4. (Color online) Dashed curves: Time series of electric field amplitude for different initial amplitudes. (a) Subcritical case,  $\gamma_d/\gamma_{L0} = 1.05$ . (b) Supercritical case,  $\gamma_d/\gamma_{L0} = 0.98$ . The other simulation parameters are given in Fig. 3. Solid line: Theoretical nonlinear instability threshold, Eq. (11).

also been explained in terms of a nonlinear reduction of ion Landau damping by particle trapping [17], which is a different mechanism.

If Krook-like collisions are negligible, then  $\gamma_{\Psi}^{\text{col}} \sim v_d^3/(k\Delta v)^2$  and  $k\Delta v_{\text{min}} \sim 0.7v_d\gamma_{L0}^{-1/3}\gamma_d^{-1/3}\omega_p^{2/3}$ . The width of the electrostatic potential well is  $4\omega_b/k$ , which is twice the width of a seed hole. Here, the electric field amplitude is measured by the bounce frequency,  $\omega_b^2 = 2k|qZ|/m$ . Thus, the initial amplitude threshold  $\omega_{b,\text{min}}$  is of the order of

$$\left( \frac{\omega_{b,\text{min}}}{\omega_p} \right)^2 \sim 0.12 \left( \frac{\omega_p}{\gamma_{L0}} \frac{\omega_p}{\gamma_d} \right)^{2/3} \left( \frac{v_d}{\omega_p} \right)^2. \quad (11)$$

Figure 4(a) shows a time series of electric field amplitude  $\omega_b$  for different initial amplitudes, for the case  $\gamma_d/\gamma_{L0} = 1.05$ , which is a subcritical instability with  $\gamma/\gamma_{L0} = -0.045$ . The threshold between damped solutions and nonlinear instabilities is in agreement with Eq. (11). We further investigate the validity of this scaling by performing a scan of  $\gamma_{L0}/\omega_p = 0.02-0.50$ ,  $\gamma_d/\gamma_{L0} = 1.01-1.20$ , and  $v_d/\gamma_{L0} = 2 \times 10^{-3}-10^{-1}$ . For each case, a series of simulations with different initial amplitudes is performed, and we measure, after one island turnover, the amplitude of the highest stable solution and the amplitude of the lowest stable solution. Figure 5 shows the range of the instability threshold, and compares it against (a) our theory, and (b) the scaling obtained in Ref. [7] in the

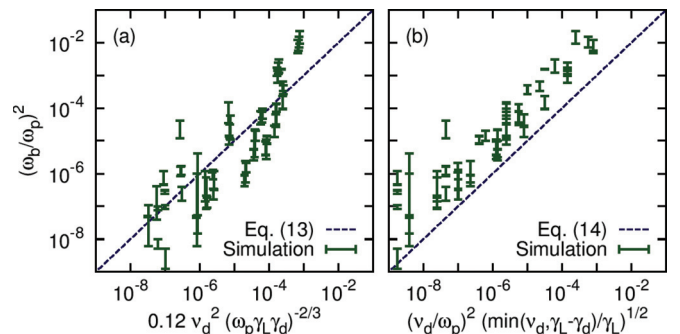


FIG. 5. (Color online) Vertical bars: Range of electric field amplitude between the highest stable and the lowest unstable simulation. Dotted line: Theory described in (a) this work and (b) Ref. [7].

limit  $\omega_b \ll \gamma_L$ ,

$$\omega_{b,\min}^2 \sim v_d^2 \max \left[ \left( \frac{v_d}{\gamma_{L0}} \right)^{1/2}, \left( \frac{|\gamma_{L0} - \gamma_d|}{\gamma_{L0}} \right)^{1/2} \right]. \quad (12)$$

Note that the two theories are not incompatible. The observed error in Fig. 5(a) is expected since Eq. (11) corresponds to a single-hole limit. The picture of Landau damping seeding the structure is valid only if the plateau shrinks slowly enough,  $|\dot{\omega}_b| \ll \omega_b^2$ . This condition must be satisfied during at least one orbit, which gives an additional condition on the initial amplitude, namely,  $\omega_b \gg (\pi + 1/2)|\gamma|$ .

In addition, our theory predicts the existence of a nonlinear instability for positive but small  $\gamma$ . For a plateau of width  $2\Delta v$ ,  $\Psi \sim \Delta v^3$  and the growth due to the linear instability is  $\Delta v/\Delta v = \gamma/2$ . Then the nonlinear instability due to phasestrophy growth is stronger than the linear growth if  $\gamma_\Psi - \gamma_\Psi^{\text{col}} > (3/2)\gamma$ . We discovered numerically the existence of such supercritical nonlinear instabilities for  $0 < \gamma/\gamma_{L0} < 0.04$ . Figure 4(b) shows a time series of electric field amplitude  $\omega_b$  for different initial amplitudes, for  $\gamma_d/\gamma_{L0} = 0.98$ , which is slightly above marginal stability with  $\gamma/\gamma_{L0} = 0.018$ . The threshold where the linear growth becomes nonlinear is in agreement with Eq. (11).

To summarize, we obtain a general relation between wave energy and phasestrophy. This relation can be applied in the BB case to obtain a simple expression for the growth rate of a single phase-space structure,  $\gamma_\Psi \sim \gamma_d \gamma_{L0} \Delta v$  in the collisionless limit. This expression shows that dissipation drives a nonlinear instability of holes and clumps via momentum exchange, regardless of linear stability. This leads to faster-than-linear growth in barely unstable regimes, as well as to subcritical instabilities, subject to the presence of a finite seed structure. Simulations in both subcritical and supercritical regimes show a good agreement with analytic theory. The extension of the present work to multiple resonances [18] would be the logical next step.

The authors are grateful for stimulating discussions with D. Escande, Y. Kosuga, C. Nguyen, and the participants in the 2009 and 2011 Festival de Théorie. This work was supported by the WCI Program of the NRF of Korea funded by the Ministry of Education, Science and Technology of Korea (WCI 2009-001), by CMTFO via US DOE Grant No. DE-FG02-04ER54738, by a grant-in-aid for scientific research of JSPF, Japan (21224014), and by the collaboration program of the RIAM of Kyushu University and Asada Science Foundation.

- 
- [1] S. Chandrasekhar, *Hydrodynamic and Hydromagnetic Stability* (Dover, New York, 1961).
- [2] P. Manneville, *Dissipative Structures and Weak Turbulence* (Springer, Berlin, 1995).
- [3] M. C. Cross and P. C. Hohenberg, *Rev. Mod. Phys.* **65**, 851 (1993).
- [4] L. D. Landau, *Dokl. Akad. Nauk SSSR* **44**, 339 (1944).
- [5] H. Schamel, *Phys. Plasmas* **19**, 020501 (2012).
- [6] T. H. Dupree, *Phys. Fluids* **25**, 277 (1982).
- [7] H. L. Berk *et al.*, *Phys. Plasmas* **6**, 3102 (1999).
- [8] M. Lesur, Y. Idomura, and X. Garbet, *Phys. Plasmas* **16**, 092305 (2009).
- [9] R. H. Berman, D. J. Tetreault, T. H. Dupree, and T. Boutros-Ghali, *Phys. Rev. Lett.* **48**, 1249 (1982).
- [10] M. Lesur *et al.*, *Nucl. Fusion* **52**, 094004 (2012).
- [11] S. I. Tsunoda, F. Doveil, and J. H. Malmberg, *Phys. Rev. Lett.* **59**, 2752 (1987).
- [12] M. Lesur *et al.*, *Phys. Plasmas* **17**, 122311 (2010).
- [13] P. H. Diamond, S. I. Itoh, and K. Itoh, *Modern Plasma Physics* (Cambridge University Press, Cambridge, UK, 2010), Vol. 1.
- [14] Y. Kosuga *et al.*, *Phys. Plasmas* **18**, 122305 (2011).
- [15] J. G. Charney and P. G. Drazin, *J. Geophys. Res.* **66**, 83 (1961).
- [16] P. H. Diamond, Y. Kosuga, and M. Lesur, *Dynamics of Structures in Configuration Space and Phase Space* (Festival de Théorie, Aix-en-Provence, 2011).
- [17] C. Nguyen, H. Lutjens, X. Garbet, V. Grandgirard, and M. Lesur, *Phys. Rev. Lett.* **105**, 205002 (2010).
- [18] D. F. Escande and Y. Elskens, *Plasma Phys. Controlled Fusion* **45**, A115 (2003).